

Contents lists available at ScienceDirect

# Physica A: Statistical Mechanics and its Applications

journal homepage: www.elsevier.com/locate/physa



# Multi-objective coordinated control strategy for mixed traffic with partially connected and automated vehicles in urban corridors



Changxin Wan<sup>a</sup>, Xiaonian Shan<sup>a,\*</sup>, Peng Hao<sup>b</sup>, Guoyuan Wu<sup>b</sup>

- <sup>a</sup> College of Civil and Transportation Engineering, Hohai University, Nanjing 210024, China
- <sup>b</sup> Center for Environmental Research & Technology, University of California at Riverside, CA 92507, USA

#### ARTICLE INFO

Keywords:
Mixed traffic flow
Connected and automated vehicle
Corridor coordinated control
Eco-driving
Signal offset optimization

# ABSTRACT

In the urban corridor with a mixed traffic composition of connected and automated vehicles (CAVs) alongside human-driven vehicles (HDVs), vehicle operations are intricately influenced by both individual driving behaviors and the presence of signalized intersections. Therefore, the development of a coordinated control strategy that effectively accommodates these dual factors becomes imperative to enhance the overall quality of traffic flow. This study proposes a bi-level structure crafted to decouple the joint effects of the vehicular driving behaviors and corridor signal offsets setting. The objective of this structure is to optimize both the average travel time (ATT) and fuel consumption (AFC). At the lower-level, three types of car-following models while considering driving modes are presented to illustrate the desired driving behaviors of HDVs and CAVs. Moreover, a trigonometry function method combined with a rolling horizon scheme is proposed to generate the eco-trajectory of CAVs in the mixed traffic flow. At the upper-level, a multi-objective optimization model for corridor signal offsets is formulated to minimize ATT and AFC based on the lower-level simulation outputs. Additionally, a revised Non-Dominated Sorting Genetic Algorithm II (NSGA-II) is adopted to identify the set of Pareto-optimal solutions for corridor signal offsets under different CAV penetration rates (CAV PRs). Numerical experiments are conducted within a corridor that encompasses three signalized intersections. The performance of our proposed eco-driving strategy is validated in comparison to the intelligent driver model (IDM) and green light optimal speed advisory (GLOSA) algorithm in single-vehicle simulation. Results show that our proposed strategy yields reduced travel time and fuel consumption to both IDM and GLOSA. Subsequently, the effectiveness of our proposed coordinated control strategy is validated across various CAV PRs. Results indicated that the optimal AFC can be reduced by 4.1%-32.2% with CAV PRs varying from 0.2 to 1, and the optimal ATT can be saved by 2.3% maximum. Furthermore, sensitivity analysis is conducted to evaluate the impact of CAV PRs and V/C ratios on the optimal ATT and AFC.

# 1. Introduction

Traffic congestion and emission have evolved into global issues due to urbanization and motorization processes. According to the United States Environmental Protection Agency (EPA), transportation activities accounted for approximately 37.5% of CO<sub>2</sub> emissions from fossil fuel consumption in 2019, primarily due to vehicle miles traveled [1]. Recently, with the advancement of intelligent

E-mail address: shanxiaonian@hhu.edu.cn (X. Shan).

<sup>\*</sup> Corresponding author.

connected and autonomous driving technologies, the emergence of connected and automated vehicles (CAVs) is widely considered to hold significant potential for enhancing urban traffic safety, efficiency, and sustainability [2–4]. However, the market penetration of CAVs will not reach 100% until 2060 s. As a result, the coexistence of a mixed traffic flow comprising both CAVs and human-driven vehicles (HDVs) is anticipated to persist well into the future [5]. Therefore, the implementation of a control strategy that guarantees the quality of future urban mixed traffic flow (e.g., efficiency, energy saving, safety) becomes a pressing necessity.

From a collective standpoint, research on traffic signal control strategies for mixed traffic flow has been studied to reduce total or average delays and fuel consumption. The core principle underlying these strategies involves the anticipation of mixed traffic flow's state information (e.g., arrival time, queue length) through the utilization of real-time CAV data. Subsequently, the signal parameters are dynamically adjusted by solving an optimization model, in which the optimization objectives are directly mapped with the state information (e.g., minimum queue length) [6–12]. For instance, Wang et al. [11] proposed a CAV-based signal control system that integrates a real-time adaptive traffic signal control at the intersection level and a dynamically coordinated control strategy at the corridor level. At the intersection level, a state information estimation method was developed based on real-time CAV data, then a real-time adaptive traffic signal control model was established to minimize the total delay at the four-legged intersection. At the corridor level, the signal offsets were dynamically adjusted to provide maximum green bandwidths to the critical pathways. The numerical results indicated that the proposed strategy can outperform the fixed coordination control system by reducing the average vehicle delay and average number of stops even with a low CAV penetration rate. Notably, at a CAV penetration rate of 100%, there was a reduction of approximately 15.7% in average vehicle delay and 13.8% in average stops.

From an individual perspective, eco-driving for CAVs is viewed as a vital approach to enhance the quality of mixed traffic flow. The fundamental concept of eco-driving is to curtail abrupt accelerations, decelerations, and idling by controlling an optimal fuel consumption trajectory for the ego CAV. Moreover, the following HDVs can be indirectly regulated through a car-following model, resulting in a reduction of the vehicular average travel time and fuel consumption. To cater the time-varying traffic conditions and the uncertain behaviors of HDVs, a Model predictive control (MPC) framework [13], also known as rolling horizon scheme, is commonly adopted to regulate the real-time optimal trajectory for the ego CAV [14–19]. For instance, Yu et al. [18] approached the trajectory optimization for the ego CAV as an optimal control problem (OCP), deducing the necessary optimal conditions based on Pontryagin's Minimum Principle (PMP), subsequently crafting a numerical method to solve the OCP. Numerical results indicated that the proposed strategy reduced the fuel consumption over than 19.37%, as the CAV penetration rate exceeded 60%.

Recently, the progress in advanced information and communication technology has enabled the realization of coordinated control within the realm of the internet of vehicles and intersections. Several studies have integrated the CAV's trajectory planning and signal optimization together, aiming to further enhance the efficiency and minimize fuel consumption within mixed traffic flow [9,20–24]. Li et al. [9] were the pioneers in suggesting the coordinated control of signal timing plans and vehicle trajectory optimization. In their study, all vehicles were assumed as CAVs, adhering to acceleration patterns governed by a rule-based eco-driving strategy. The signal timing plan, aimed at minimizing overall delay, was established through an exhaustive method. Jung et al. [20] developed a bi-level optimization method for an eco-traffic signal system that integrates an eco-driving algorithm and an eco-signal operation at an isolated intersection. The upper-level optimized the setting of signal timing plan that minimized the total delays, while the lower level controlled the optimal fuel consumption trajectory of CAVs by solving a nonlinear programming problem. The penetration rate of CAV was also assumed 100%. A Similar methodology was also adopted by Xu et al. [21]. For mixed traffic flow scenarios, Yao et al. [22] developed a two-level framework that optimized both isolated intersection traffic signals and vehicle trajectories. At the vehicle level, a model predictive control framework was proposed to optimize vehicle trajectories while considering gasoline consumption. At the intersection level, dynamic programming was applied to optimize traffic signal timing, utilizing predicted vehicle arrival determined by the lower level. Tajalli and Haijbabaie [23] formulated the joint signal timing and trajectory control as a mixed-integer non-linear program (MILP) for isolated intersection, linearization of the objective function and nonlinear constraints was implemented to reduce the complexity of the MILP problem, then the Lagrangian relaxation technique was used to decompose the programming problem to several sub-problems as a balance between computational efficiency and solution equality. Considering the cooperation of intersections, Yang et al. [24] proposed a hierarchical cooperative driving framework with a mixed traffic composition of CAVs, connected vehicles (CVs), and HDVs for urban corridors. The framework consisted of three levels of models. At the vehicle level, a state transition mechanism was designed to differentiate the operations of CAVs encompassing eco-trajectory planning, cooperative adaptive cruise control (CACC), and collision avoidance. At the intersection level, a MILP problem was established to optimize the signal timing plan along with the arrival time of CAVs while considering CAV platoons. At the corridor level, link performance functions are employed to calculate the overall delay of the coordinated phases at each intersection and a linear programming (LP) problem is formulated to optimize the signal offsets for every cycle.

Although researches have been made in the region of the coordinated control strategy consist of eco-driving and signal optimization, existing studies are fraught several limitations. First, the driving mode is rarely accounted for within the eco-driving strategy, resulting in an absence of differentiation in the eco-driving approach when a CAV follows a HDV or another CAV [14,18,21,22,25]. However, in instances where a CAV follows a CAV, the ego CAV can achieve cooperative control through vehicle-to-vehicle (V2V) communication, thereby rendering the eco-driving strategy more adaptable and efficacious [16,24]. Second, many existing studies of the coordinated control strategy focus on an isolated intersection, without considering the cooperation between intersections [9, 20–23]. Finally, a single-objective optimization model (e.g., minimum total delays, maximum outflow rate), or an optimization model that weighted summarizes the objectives were commonly used in signal optimization [9,20–24]. However, the objectives may conflict with each other (e.g., minimize total delays versus maximize traffic flow safety), and the trade-off is hard to determine for objectives with different units. Therefore, a multi-objective optimization model that draws the Pareto-optimal frontier of objectives is imperative to establish.

Realizing the research gaps, this study proposes a multi-objective coordinated control strategy in urban corridors for mixed traffic consisting of HDVs and CAVs. A bi-level structure is designed to decouple the interaction of the signal offset optimization and ecological trajectory planning of CAVs, as informed by previous studies [20–22]. In the structure, the lower-level simulates the trajectory of HDVs and CAVs with the implementation of a driving mode based eco-driving strategy. The upper-level optimizes the corridor signal offsets that minimize the average travel time and fuel consumption, both of which can be determined by the simulation of lower-level. Then, a revised Non-Dominated Sorting Genetic Algorithm II (NSGA-II) is developed to achieve a set of Pareto-optimal solutions for corridor signal offsets, as well as the trajectories of HDVs and CAVs. Finally, the effectiveness of the proposed coordinated control strategy is discussed through microscopic simulation.

The main contributions of this study are summarized as follows:

- (1) designs a bi-level structure that decouples the interaction of the corridor signal offsets optimization and CAV's ecological trajectory planning, and proposes an eco-driving strategy for CAVs in the mixed traffic flow while considering the driving modes.
- (2) establishes a multi-objective optimization model for corridor signal offsets that minimizes the average travel time and fuel consumption of vehicles, and develops a revised NSGA-II that obtains the Pareto-optimal solutions of the multi-objective optimization model.
  - (3) analyses the effectiveness of the proposed coordinated control strategy with different CAV PRs and V/C ratios.

The remaining structure of this paper is organized as follows. Section 2 describes the addressed problem. Section 3 designs the trajectory generation method for HDVs and CAVs with the implementation of eco-driving. Section 4 formulates the multi-objective optimization model for corridor signal offsets, and proposes a revised NSGA-II to solve the optimization model. Section 5 conducts numerical experiments and sensitivity analysis. Section 6 presents the conclusions, research limitations and future work directions.

## 2. Problem description and notations

## 2.1. Problem description

As illustrated in Fig. 1, this study focuses on an urban corridor consisting of multiple signalized intersections. Within this context, two types of vehicles are considered, i.e., HDVs and CAVs. All vehicles travel straight through the intersections within the corridor, without performing any turning movements such as left-turns or right-turns. Notably, each intersection is conceptualized as a single-lane roadway, thereby overtaking and lane-changing behaviors are prohibited for all vehicles. For each intersection, the setting of Signal Phase and Timing (SPaT) is assumed as uniform. There is a control center in the corridor that can simulate the trajectories of HDVs and CAVs, calculating the average travel time and fuel consumption by using the trajectories, then optimizing the corridor signal offsets based on these indicators. Moreover, for each intersection within the corridor, a sub-control center is in place. This sub-control center has the capacity to receive real-time vehicle dynamic states (e.g., position, and speed) and SPaT information by roadside units (RSUs). Utilizing these data, the sub-control center offers acceleration guidance to CAVs for the purpose of eco-driving.

During the implementation of the CAVs' eco-driving strategy, note that the preceding vehicle of the ego CAV can either be a HDV or a CAV. Thus, the implementation of eco-driving strategy should consider the driving mode (i.e., ego CAV following HDV, ego CAV following CAV). Moreover, it is noteworthy that the eco-driving strategy might encounter challenges, such as an inability to derive a viable acceleration profile or the potential for collision with the preceding vehicle. To address these concerns, a rolling horizon scheme is applied to ensure efficiency and safety, similar to the philosophy in MPC [26].

For the optimization of corridor signal offsets, there are two objectives (i.e., the average travel time and fuel consumption) that represent the efficiency and sustainability of the mixed traffic flow, which are inherently challenging to transform into directly comparable units. Therefore, a multi-objective optimization model is selected to obtain the Pareto optimal solutions, instead of single-objective or multi-objective weighted summation optimization model.

However, the effectiveness of corridor signal offsets optimization is subject to alteration upon the implementation of CAV's ecological trajectory planning. At the same time, the performance of the eco-driving strategy is also influenced by the corridor signal

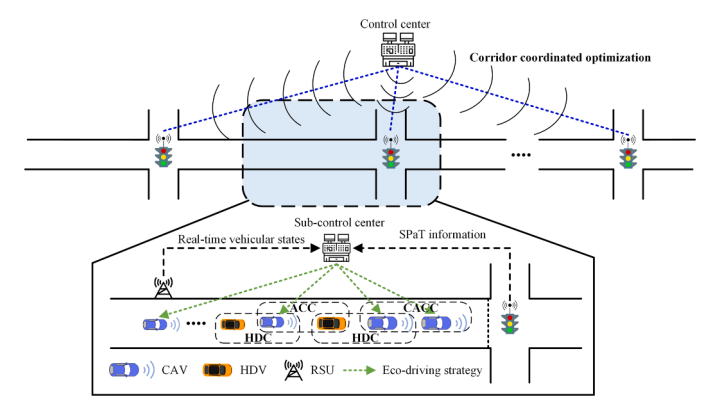


Fig. 1. The coordinated control strategy for mixed traffic in an urban corridor.

offsets setting. To decouple the interaction of the corridor signal offsets optimization and CAV's ecological trajectory planning, a bilevel structure is designed as shown in Fig. 2. With the determined roadway (i.e., Number of intersections, setting of signal phase and timing) and mixed traffic flow (i.e., V/C ratio, CAV penetration rate) parameters. At the lower level, the trajectories of HDVs and CAVs with the implementation of a driving mode based eco-driving strategy are simulated to obtain average travel time  $f_t$  and fuel consumption  $f_e$  as a vector f, for given corridor signal offsets  $\phi$ . At the upper-level, a multi-objective optimization for corridor signal offsets  $\phi$  is solved to get the set of Pareto-optimal solutions, for given objective vector f. Through repeated iterations of this bi-level structure, the set of Pareto-optimal solutions for corridor signal offsets, and the trajectories of HDVs and CAVs are obtained finally.

#### 2.2. Notations

Main notations applied hereafter are summarized in Table 1.

# 3. Lower-level: trajectory generation for HDVs and CAVs

In this section, the trajectory generation method under mixed traffic environment is introduced. First, three types of driving modes and corresponding car-following models are classified to depict the heterogeneous characteristics of HDVs and CAVs. Second, a trajectory generation method for HDVs is proposed while considering the lack of SPaT information. Third, a driving mode based ecodriving strategy combined with rolling horizon scheme is designed to optimize the speed profile of CAVs in situations where it cannot pass through the adjacent intersection as its current desired acceleration and SPaT information. Finally, a framework of lower-level problem is introduced to simulate the whole trajectories for given upper-level parameters.

#### 3.1. Driving mode classification for HDV and CAV

As shown in Fig. 1, there are three driving modes under mixed traffic environment, HDC (Human-driven control, HDV following HDV or CAV), ACC (Adaptive cruise control, CAV following HDV), and CACC (Cooperative Adaptive cruise control, CAV following CAV). HDC mode represents the human-driven behavior that cannot interact with RSUs and preceding vehicles. ACC and CACC are typical driving modes for CAVs. ACC utilizes onboard detection equipment to obtain information (e.g., speed, position) of the preceding vehicles, enabling acceleration control optimization. CACC, which builds upon ACC, leverages V2V communication technology to exchange information with preceding vehicles, thereby forming CAV platoons and achieving collaborative control [27]. To address the heterogeneous characteristics of these driving modes, the intelligent driver model (IDM) with different desired time headway is employed in this study [28–30]. The IDM acceleration  $a_n^a(t)$  of the n-th vehicle at time t is calculated using the following formula:

$$a_n^d(t) = f_n(v_n(t), \Delta v_n(t), s_n(t)) = a_{\text{max}} \left[ 1 - \left( \frac{v_n(t)}{v_{\text{max}}} \right)^4 - \left( \frac{s_n^*(t)}{s_n(t)} \right)^2 \right]$$
 (1)

$$s_n^*(t) = s_0 + \max \left\{ 0, v_n(t) T_n + v_n(t) \Delta v_n(t) / \left( 2\sqrt{|a_{\text{max}} a_{\text{comf}}|} \right) \right\}$$
 (2)

where  $a_{\max}$ ,  $a_{comf}$  represent the maximum and comfortable deceleration.  $v_{\max}$  is the maximal limit speed.  $s_0$  denotes the jam gap.  $T_n$  represents the desired time headway, which can be  $T_{hdc}$ ,  $T_{acc}$  or  $T_{cacc}$  related to driving control mode, satisfies  $T_{hdc} \geq T_{acc} \geq T_{cacc} \cdot v_n(t)$  is the current speed of the n-th vehicle.  $\Delta v_n(t)$  is the speed error to the preceding vehicle n-1,  $\Delta v_n(t) = v_n(t) - v_{n-1}(t)$ .  $s_n(t)$  and  $s_n^*(t)$  represent the actual and desired safe space gap,  $s_n(t) = x_{n-1}(t) - x_n(t) - l$ . l represents the length of vehicle,  $f_n(v_n(t), \Delta v_n(t), s_n(t))$  is the general form of the IDM.

 $a_n^d(t)$  represents the desired acceleration of the ego vehicle without other interference. However, on urban roads, the acceleration of HDVs and CAVs is not only affected by the preceding vehicle and itself, the traffic lights at the nearest intersection also play a significant role. If the ego vehicle is a HDV, it may come to a stop at the intersection due to a red signal phase. On the other hand, if the ego vehicle is a CAV in ACC driving mode, it has the capability to regulate its real-time speed based on the received information of preceding HDV's current state and intersection's SPaT, reaching the optimization of travel time and fuel consumption. In cases where the

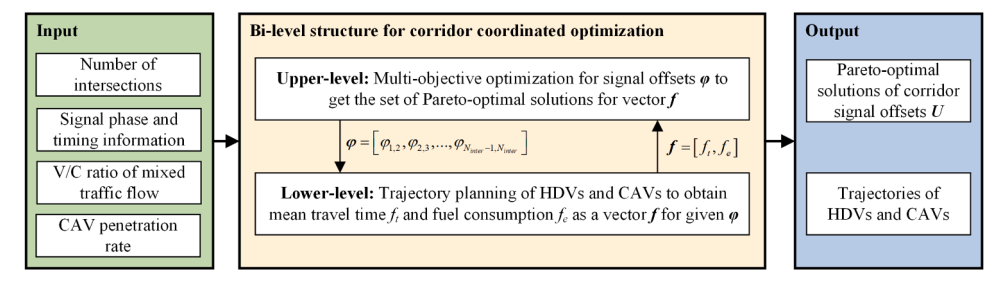


Fig. 2. The bi-level structure of the coordinated control strategy.

Table 1
Notations.

Variables	Meaning	Unit
General Notations		
i	Intersection index	
n	Vehicle index	
k	Iteration index of the rolling horizon scheme	
j	Chromosome index	
w	Iteration index of the revised NSGA-II	
d	Level index of non-dominated solution set	
Lower-level problem pa	arameters	
Vehicle parameters		
$x_n(t)$	Position of the <i>n</i> -th vehicle at time t	m
$s_n(t)$	Space gap between the <i>n</i> -th vehicle and its preceding vehicle <i>n</i> -1	m
$s_n^*(t)$	Desired space gap between the <i>n</i> -th vehicle and its preceding vehicle <i>n</i> -1	m
$s_0$	Jam gap between two consecutive vehicles	m
$t_n^{L_i}$	Passage time when the $n$ -th vehicle reach the stop bar of intersection $i$	s
	Predicted passage time when the $n$ -th vehicle reach the stop bar of intersection $i$	s
$\widehat{t}_n^{L_i}$		
$v_n(t)$	Speed of the <i>n</i> -th vehicle at time <i>t</i>	m/s
$\Delta v_n(t)$	Speed error between the <i>n</i> -th vehicle and its preceding vehicle <i>n</i> -1	m/s
$v_{max}$	Maximum limit speed	m/s
$a_{\min}$	Minimum acceleration	m/s <sup>2</sup>
$a_{\max}$	Maximum acceleration	$m/s^2$
$a_{comf}$	Comfortable deceleration	m/s <sup>2</sup>
$a_n(t)$	Actual acceleration of the $n$ -th vehicle at time $t$	$m/s^2$
$a_n^d(t)$	Desired (safe) acceleration of the $n$ -th vehicle at time $t$	m/s <sup>2</sup>
$a_n^{L_i}(t)$	Acceleration affected by nearby stop bar of the n-th vehicle at time <i>t</i>	m/s <sup>2</sup>
$G_n(t)$	Acceleration profile calculated by trigonometry method of the <i>n</i> -th vehicle at time <i>t</i>	$m/s^2$
$a_n^r(t)$	Replaced acceleration if trigonometry method cannot find a feasible solution; $G_n(t) = \emptyset$	$m/s^2$
		m/s <sup>3</sup>
k <sub>max</sub>	Maximum change rate of acceleration	III/S
Intersection parameter		
$L_i$	Position of the stop bar of intersection i	m
$G_i$	Set of green phases of intersection i	S
$Y_i$	Set of yellow phases of intersection <i>i</i>	S
$R_i$	Set of red phases of intersection i	S
$\Omega_i$	Set of green and yellow phase of intersection $i$ ; $\Omega_i = G_i \bigcup Y_i$	S
$t_C$	Duration of signal cycle	S
$t_G$	Duration of green phase	S
$t_Y$	Duration of yellow phase	S
$t_R$	Duration of red phase	S
$t_{ls}$	Lost time of vehicle's start up	S
Upper-level problem pa	arameters	S
N <sub>inter</sub>	Number of intersections	
$\varphi_{i,i+1}$	Offset of the signal phase from intersection $i$ to intersection $i+1$	
$\varphi$	Vector of corridor signal offsets; $\boldsymbol{\varphi} = [\varphi_{1,2}, \varphi_{1,3}, \varphi_{N_{inter}-1,N_{inter}}]$	s
$f_t(\varphi)$	Average travel time of vehicles for given signal offsets $\varphi$	s
$f_e(\varphi)$	Average fuel consumption of vehicles for given signal offsets $\varphi$	s/veh
$f(\varphi)$	Vector of objective functions for given signal offsets $\varphi$ ; $f(\varphi) = [f_t, f_e]$	mL/ve
<b>Μ</b>	Size of populations in the revised NSGA-II	IIIL/ VC
W	Maximum iteration of the revised NSGA-II	
$p_c, p_m$	Probabilities of crossover and mutation in the revised NSGA-II	
$U_w$	Parent population in the <i>w</i> -th iteration	
$V_w$	Child population in the <i>w</i> -th iteration	
$Z_w$	Merged population in the <i>w</i> -th iteration; $\mathbf{Z}_w = \mathbf{U}_w \bigcup \mathbf{V}_w$	
$R_d$	Pareto-optimal solutions set of the <i>d</i> -th level.	
$D_{id}$	Crowd distance of the <i>j</i> -th chromosome in the <i>d</i> -th non-dominated solution level	

ego CAV adopts the CACC driving mode, it can not only receive the current state information of the preceding vehicle, but also directly acquire the predicted trajectory of the preceding CAV, achieving cooperative driving control.

# 3.2. Trajectory generation for HDVs

Fig. 3. depicts the trajectory generation scheme for HDV n at intersection i within each time step  $\Delta t$ . The HDV will maintain the desired acceleration calculated by Eqs. (1) and (2), if the vehicle can pass the signalized intersection during the green or yellow phase. However, if the HDV cannot pass the intersection or the ongoing signal phase is red, it will come to a stop before reaching the stop bar [25]. Therefore, at the start time  $t_0$ , the HDV needs to calculate the desired terminal time for passing through intersection i, based on its current state and desired acceleration. In this study, three acceleration values are identified to calculate the desired passage time  $t_n^{L_i}$ : (1)  $a_n^d(t_0) > 0$ ; (2)  $a_n^d(t_0) = 0$ ; and (3)  $a_n^d(t_0) < 0$ .

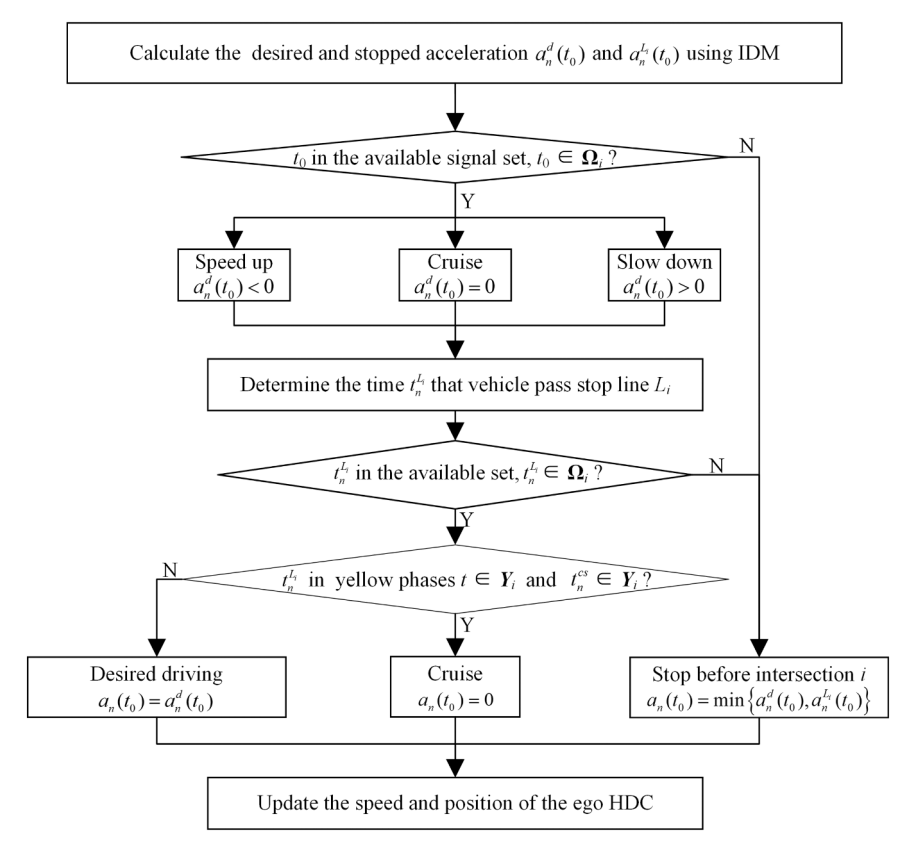


Fig. 3. The control scheme of HDVs.

(1)  $a_n^d(t_0) > 0$ , the desired passage time  $t_n^{L_i}$  can be divided into two cases (reach to maximum speed or not), which is calculated as follows:

$$t_{n}^{L_{i}} = \begin{cases} t_{0} + \frac{\sqrt{v_{n}^{2}(t_{0}) + 2a_{n}^{d}(t_{0}) \times (L_{i} - x_{n}(t_{0}))} - v_{n}(t_{0})}{a_{n}^{d}(t_{0})}, \ x_{n}^{acc} \ge L_{i} \\ t_{0} + t_{n}^{acc} + \frac{2(L_{i} - x_{n}(t_{0})) - t_{n}^{acc} \times (v_{n}(t_{0}) + v_{\max})}{2v_{\max}}, \ x_{n}^{acc} < L_{i} \end{cases}$$

$$(3)$$

where  $x_n^{acc}$  is the position HDC accelerates to maximum speed, satisfies  $x_{n,acc} = x_n(t_0) + \frac{v_{\max}^2 - v_n^2(t_0)}{2d_n^2(t_0)}$ .  $t_n^{acc}$  is the acceleration time from current speed  $v_n(t_0)$  to the limit speed  $v_{\max}$ ,  $t_n^{acc} = \frac{v_{\max} - v_n(t_0)}{a_n^d(t_0)}$ .

(2)  $a_n^d(t_0) = 0$ ,  $t_n^{L_i}$  is calculated as follows:

$$t_n^{L_i} = t_0 + t_n^{cs} = t_0 + \frac{L_i - x_n(t_0)}{v_n(t_0)}$$
(4)

where  $t_n^{cs}$  represents the time that HDV drives from  $x_n(t_0)$  to stop bar  $L_i$  as a speed of  $v_n(t_0)$ .

(3)  $a_n^d(t_0) < 0$ , the passage time  $t_n^{l_i}$  can also be divided into two cases (decelerates to zero or not), which is calculated as follows:

$$t_{n}^{L_{i}} = \begin{cases} t_{0} + \frac{\sqrt{v_{n}^{2}(t_{0}) + a_{n}^{d}(t_{0}) \times (L_{i} - x_{n}(t_{0}))} - v_{n}(t_{0})}{a_{n}^{d}(t_{0})}, x_{n}^{dec} \ge L_{i} \\ \infty, x_{n}^{dec} < L_{i} \end{cases}$$
(5)

where  $x_n^{dec}$  is the position HDC decelerates to zero, satisfies  $x_n^{dec} = x_n(t_0) - \frac{y_n^2(t_0)}{2a_n^d(t_0)}$ .  $t_n^{dec}$  is the acceleration time from current speed  $v_n(t_0)$  to zero,  $t_n^{dec} = \frac{-v_n(t_0)}{a_n^d(t_0)}$ .

Based on desired passage time and the SPaT information at the intersection i, the acceleration of the ego HDV can be ascertained. If  $t_n^{L_i} \notin \Omega_i$  or  $t_0 \notin \Omega_i$ , the HDV should stop before the stop bar. To ensure safety, the acceleration of the HDV must be neither lower than

car-following acceleration  $a_n^l(t_0)$  nor stopped acceleration  $a_n^{l_l}(t_0)$ . The stopped acceleration  $a_n^{l_l}(t_0)$  is calculated as follows:

$$a_n^{L_i}(t_0) = a_{\max} \left[ 1 - \left( \frac{v_n(t_0)}{v_{\max}} \right)^4 - \left( \frac{s_0 + \max\{0, v_n(t_0)T_n + v_n^2(t_0) / (2\sqrt{|a_{\max}a_{comf}|})\}}{L_i - x_n(t_0)} \right)^2 \right]$$
 (6)

If  $t_0 \in \Omega_i$  and  $t_n^{t_i} \in \Omega_i$ , i.e., the HDV can pass the stop bar  $L_i$  before red phase, it will maintain the desired acceleration  $a_n^d(t_0)$ . Particularly, if  $t_n^{t_i} \in Y_i$  and the HDV can pass the stop bar  $L_i$  as the current speed  $v_n(t_0)$  ( $t_n^{cs} \in Y_i$ ), the acceleration of such HDV will be set to zero while considering safety and comfortably. Hence, the acceleration of HDV can be determined as follows:

$$a_n(t_0) = \begin{cases} \min\{a_n^d(t_0), a_n^{L_i}(t_0)\}, & \text{if } t_0 \notin \Omega_i \text{or } t_n^{L_i} \notin \Omega_i \\ a_n^d(t_0), & \text{if } t_0 \in \Omega_i, t_n^{t_n} \in \Omega_i, t_n^{cs} \notin Y_i \\ 0, & \text{otherwise} \end{cases}$$

$$(7)$$

The position and speed of the HDV at next step  $(t_0 + \Delta t)$  can be updated as follows:

$$v_n(t_0 + \Delta t) = v_n(t_0) + a_n(t_0)\Delta t \tag{8}$$

$$x_n(t_0 + \Delta t) = x_n(t_0) + \frac{\Delta t}{2}(v_n(t_0) + v_n(t_0 + \Delta t))$$
(9)

Using Eqs. (7)–(9) repeatedly, the trajectory of HDV at each intersection can be derived.

#### 3.3. Eco-driving strategy for CAVs

CAVs have an advantage over HDVs in situations where the desired acceleration is not feasible. Leveraging SPaT information and state data from the preceding vehicle, CAVs can predict the passage time  $\hat{t}_n^{L_i}$  of the nearest intersection. Based on the predicted passage time  $\hat{t}_n^{L_i}$ , CAVs can generate an ecological trajectory that allows them to pass through the current intersection without stopping. The eco-driving strategy for CAVs consists of two parts: (1) passage time prediction and (2) eco-acceleration generation. A scheme is proposed to outline the process of these components, as shown in Fig. 4.

## 3.3.1. Passage time prediction

In the passage time prediction, two cases are considered: one where there exists a vehicle in front of the ego CAV, and the other where there is not. In the absence of a preceding vehicle, the ego CAV can pass the stop bar at the earliest arrival time or the starting time of the next green phase,  $\hat{t}_n^{L_i} = \max\left\{\left|\frac{t_0}{t_C}\right| t_C + \varphi_{i-1,i}\right|_{i>1}, t_0 + \frac{L_i - x_n(t_0)}{v_{\max}} + \frac{(v_{\max} - v_n(t_0))^2}{2v_{\max}a_{\max}}\right\}$ .

When there are vehicles ahead of the ego CAV,  $\hat{t}_n^{I_i}$  is determined based on its preceding vehicles and SPaT information. If the preceding vehicle is a CAV, the ego CAV is at CACC driving mode, it can directly acquire the passage time of the preceding CAV. On the

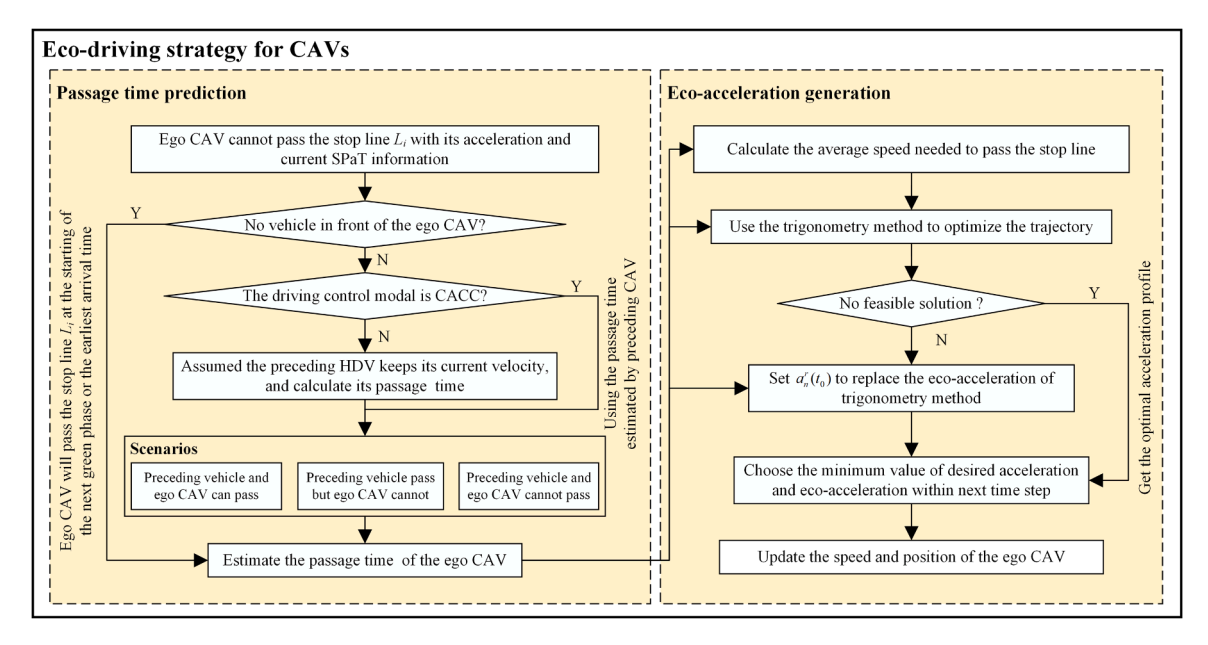


Fig. 4. The eco-driving strategy for CAVs.

other hand, if the preceding vehicle is a HDV, an assumption is made that the speed of the leading HDV remains constant [19]. Consequently, the predicted passage time  $\tilde{t}_{n-1}^{L_i}$  that the preceding vehicle passing through the stop bar can be determined using the following formula:

$$\widetilde{t}_{n-1}^{L_i} = \begin{cases}
\chi t_{n-1}^{L_i} + (1-\chi) \widetilde{t}_{n-1}^{L_i}, & \text{ifCACC} driving mode} \\
t_0 + \frac{x_{sl} - x_{n-1}(t_0)}{v_{n-1}(t_0)}, & \text{otherwise}
\end{cases} (10)$$

where  $\chi$  is a binary decision variable,  $\chi=1$  when  $t_{n-1}^{I_i}\in \Omega_i$ , else  $\chi=0$ .

Based on the current SPaT information and  $\hat{t}_{n-1}^{L_i}$ ,  $\hat{t}_n^{L_i}$  can be calculated as follows:

$$\hat{t}_{n}^{L_{i}} = \begin{cases}
\hat{t}_{n-1}^{L_{i}} + t_{hw}, \hat{t}_{n-1}^{L_{i}} \in \left[ \left( \left\lceil \frac{\hat{t}_{n-1}^{L_{i}}}{t_{C}} \right\rceil - 1 \right) t_{C}, t_{r} - t_{hw} \right] \cup \left[ \left\lceil \frac{\hat{t}_{n-1}^{L_{i}}}{t_{C}} \right\rceil t_{C}, t_{r}' - t_{hw} \right] \\
\left[ \frac{\hat{t}_{n-1}^{L_{i}}}{t_{C}} \right] t_{C}, \hat{t}_{n-1}^{L_{i}} \in \left[ t_{r} - t_{hw}, t_{r} \right] \cup \left[ t_{r}' - t_{hw}, t_{r}' \right] \\
\left[ \frac{\hat{t}_{n-1}^{L_{i}}}{t_{C}} \right] t_{C} + t_{ls} + N_{p} t_{hw}, \hat{t}_{n-1}^{L_{i}} \in \left[ t_{r}, \left\lceil \frac{\hat{t}_{n-1}}{t_{C}} \right\rceil t_{C} \right] \cup \left[ t_{r}', \infty \right]
\end{cases}$$
(11)

where  $t_{hw}$  is the saturation time headway, which equals to the reciprocal of IDM maximum volume.  $t_r$  is the time with current signal phase turning to red,  $t_r = \left(\frac{\left\lceil \frac{t_{l-1}}{t_C}\right\rceil}{t_C} - 1\right)t_C + t_R + t_Y$ .  $t_r'$  is the time with the next signal phase turning to red,  $t_r = \left\lceil \frac{t_{l-1}}{t_C}\right\rceil t_C + t_R + t_Y$ .  $t_l'$  is the start time at the beginning of green phase.  $N_p$  is the number of preceding vehicles with respect to current CAV before the stop bar.

The first branch in Eq. (11) addresses the scenario where both the current and preceding vehicle can pass through stop bar before the red phase,  $\hat{t}_n^{L_i}$  is set as  $\hat{t}_{n-1}^{L_i} + t_{hw}$  to ensure vehicle travel efficiency. The second condition covers situation where the preceding vehicle can pass through stop bar before the red phase, while the current CAV cannot do so in time,  $\hat{t}_n^{L_i}$  is equal to  $\begin{bmatrix} t_0 \\ t_C \end{bmatrix} t_C$ . The last branch deals with the case that the preceding vehicle cannot reach the stop bar before red phase, and there are  $N_p$  number of vehicles in front of the preceding vehicle, where  $\hat{t}_n^{L_i}$  is set to  $\begin{bmatrix} t_0 \\ t_C \end{bmatrix} t_C + t_{ls} + N_p \times t_{hw}$ .

# 3.3.2. Eco-acceleration generation

The trigonometry function method [31] is selected to generate the ecological trajectory of CAVs while considering the computational efficiency, outlined as follows:

$$v_{n}(t) = \begin{cases} v_{h} + v_{d} \cos\left(st\right), & t \in \left[t_{0}, t_{0} + \frac{\pi}{2s}\right) \\ v_{h} + \frac{s}{a}v_{d} \cos a\left(t - \frac{\pi}{2s} + \frac{\pi}{2a}\right), & t \in \left[t_{0} + \frac{\pi}{2s}, t_{0} + \frac{\pi}{2s} + \frac{\pi}{2a}\right) \\ v_{h} + \frac{s}{a}v_{d}, & t \in \left[t_{0} + \frac{\pi}{2s} + \frac{\pi}{2a}, \hat{t}_{n}^{L_{i}}\right) \end{cases}$$

$$(12)$$

where  $v_h$  is the average speed at time period t, calculated by  $v_h = \min \left\{ v_{\max}, \frac{L_l - x_n(t_0)}{\lambda_l} \right\}$ .  $v_d$  is the speed difference between the current speed  $v_n(t_0)$  and the average speed  $v_h$ , calculated by  $v_d = v_n(t_0) - v_h$ . (s, a) control the rate of change of acceleration, different values of (s, a) show the different acceleration and jerk profiles.

Based on previous research [31] to minimize energy consumption, parameter s should be chosen as large as possible, with the temporal-spatial, vehicle acceleration and jerk constraints, s is determined by an optimization model as follows:

$$\max_{s \in (0,1]} \{s\} \tag{13}$$

Subject to:

$$x_n(t_0) + \int_{t_0}^{t_n^{L_i}} v_n(t)dt = L_i$$
 (14)

$$0 \le v_n(t) \le v_{\text{max}}, \forall t \in \left(t_0, \hat{t}_n^{L_i}\right]$$

$$\tag{15}$$

$$a_{\min} \le a_n(t) \le a_{\max}, \forall t \in \left(t_0, \hat{t}_n^{L_i}\right)$$
 (16)

$$|da_n(t)/dt| \le k_{\max}, \forall t \in \left(t_0, \hat{t}_n^{L_i}\right]$$
(17)

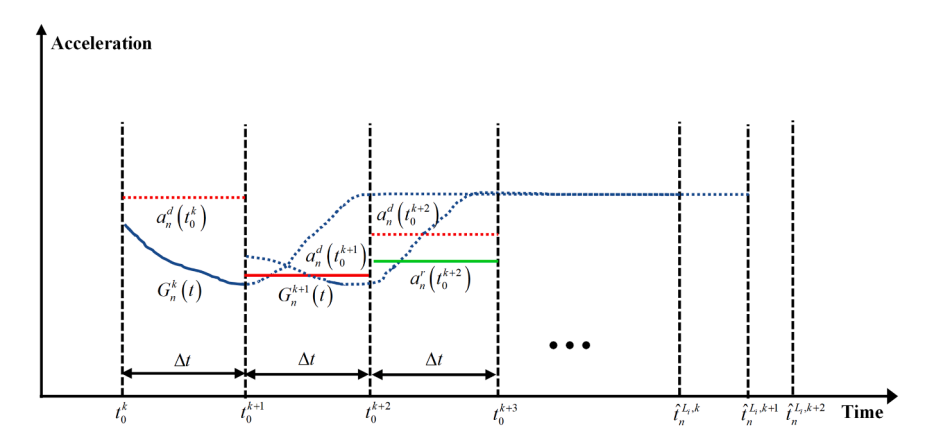


Fig. 5. The rolling horizon scheme of CAV's eco-driving.

where  $k_{\text{max}}$  is the maximum change rate of acceleration, respectively. Eq. (14) states that the CAV passes the stop bar at time of  $\hat{t}_n^{L_i}$ . Eqs. (15), (16), and (17) limit the boundary of speed. acceleration and the jerk, respectively. Note that there are two variables in one equation. Therefore, for a given s, a can be calculated using Eq. (14). Discretized with interval of 0.01, s can be easily solved by exhaustive method. Once the pair of (s, a) is ascertained, the trajectory of CAV n can be derived employing Eq. (12).

However, it is worth noting that the trigonometry method outlined in Section 3.3.2 may not always yield a feasible (s,a) pair under some extreme conditions, and it might not effectively prevent crashes among vehicles if only employed once. To address these challenges, a rolling horizon scheme is devised, as illustrated in Fig. 5. The solid line depicts the acceleration implemented over each time step  $\Delta t$ , and the dashed line denotes the unaccepted acceleration. In scenario where the trigonometry method yields a feasible (s,a) pair, the eco-trajectory  $G_n^k(t) = dv_n(t)/dt$  is generated at the start time  $t_0^k$  of each iteration k for a time period  $[t_0^k, \hat{t}_n^{L_i,k}]$ . It is important to make the actual acceleration remains below the car-following acceleration  $a_n^t(t_0^k)$  to ensure driving safety. On the other hand, in situation where the (s,a) pair is infeasible, an approximate acceleration  $a_n^r(t_0^k)$  is chosen to as a substitute for  $G_n^k(t)$ . In that case, the actual acceleration also should be chosen as the minimal value of  $a_n^r(t_0^k)$  and  $a_n^d(t_0^k)$  In essence, the actual acceleration adopted by the ego CAV in time period  $[t_0^k, t_0^{k+1}]$  ( $t_0^{k+1} = t_0^k + \Delta t$ ) is as follows:

$$a_{n}^{k}(t) = \begin{cases} \min\{a_{n}^{d}(t_{0}^{k}), a_{n}^{r}(t_{0}^{k})\}, if G_{n}^{k}(t) \in \emptyset \\ \min\{a_{n}^{d}(t_{0}^{k}), G_{n}^{k}(t)\}, otherwise \end{cases}$$
(18)

where  $a_n^d(t_0^k)$  is the car-following acceleration calculated by Eq. (1).  $a_n^r(t_0^k)$  is the minimal acceleration needed from current speed  $v_n(t_0^k)$  to the average speed  $(v_h^k)$  of the n-th CAV,  $a_n^r(t_0^k) = \max\{a_{\min}, \frac{1}{\Delta t}(v_h^k - v_n(t_0^k))\}$ .

Without considering the lane change behavior of the CAV, the position and speed of CAV at next time  $t_0^{k+1}$  are determined as follows:

$$v_n(t_0^{k+1}) = \int_{t_0^k}^{t_0^{k+1}} a_n^k(t)dt, x_n(t_0^{k+1}) = \int_{t_0^k}^{t_0^{k+1}} v_n(t)dt$$
(19)

By Iteratively applying Eqs. (10)-(19), the trajectory of the CAV implementation with eco-driving strategy at each signalized intersection can be obtained.

#### 3.4. Simulation framework of the lower-level problem

**Algorithm 1.** depicts the simulation framework of the lower-level problem. The corridor road information (number of intersections, length of each intersection) and signal parameters (SPaT and corridor signal offsets) are pre-defined. The total number of vehicles (CAVs and HDVs) is determined for given V/C ratio, CAV penetration rate, and simulation time horizon. During each time step, the acceleration of each HDV is generated by the control scheme in Section 3.2, and the movement for one CAV follows the eco-driving strategy in Section 3.3. After the simulation, all the vehicles' information (including position, speed, and acceleration) in the urban corridor are recorded to calculate the travel time and fuel consumption for the upper-level optimization.

# **Algorithm 1**. The simulation of lower-problem.

```
Input: The number of intersections N_{inter}, position of stop bar for each intersection L;
        The signal parameters of intersections [G, Y, R], corridor signal offsets \varphi:
        The simulation time horizon T_{sim}, the V/C ratio \gamma, CAV penetration rate \lambda.
1: Set time t = 0, \Delta t = 1, the total number of vehicles N_{sim} = \frac{t_G + t_Y - t_{ls}}{\gamma t_{c} t_{loc}} T_{sim}, the number of vehicles enter each
  intersection N_{enter} = 0 , and the number of vehicles passes the stop bar of each intersection N_{pass} = 0.
2: while \min\{N_{pass}\} \leq N_{sim} do
     ## collect the number of vehicles at each intersection at each time
      for i = 1, 2, ..., N_{inter} do
4:
5:
       if a new vehicle comes at i-th intersection at time t then
         N_{enter,i} = N_{enter,i} + 1 and collect vehicle's initial state x_n(t), v_n(t).
6:
7:
8:
      ## update the position and speed of each vehicle, and the inflow and outflow information of each intersection
9:
      for i = 1, 2, ..., N_{inter} do
10:
         for n = 1, 2, ..., N_{enter,i} do
11:
            if the n-th vehicle is a HDV then
12:
                                                                                                   # acceleration generation for HDV
             Use the control scheme illustrated in Section 3.2 to get the acceleration a_n(t).
13:
14:
            else if the n-th vehicle is a CAV then
                                                                                                        # eco-driving strategy for CAV
             Use the eco-driving strategy established in Section 3.3 to get the eco-acceleration a_n(t).
15:
16:
17:
            Update vehicle's state x_n(t), v_n(t) based on a_n(t).
            if x_n(t) > L_i then
18:
                                                                                        # the n-th vehicle passes the i-th intersection
             \begin{split} N_{enter,i} &= N_{enter,i} - 1 \; . \\ N_{pass,i} &= N_{pass,i} + 1 \; . \end{split}
19:
20:
21:
22:
         end for
23:
      end for
24: Set t = t + \Delta t.
25: end while
Output: the total trajectory of each vehicle [x_n, v_n, a_n], n = 1, 2, ..., N_{sim}.
```

# 4. Upper-level: multi-objective optimization for corridor signal offsets

The upper-level problem focuses on the corridor signal offset optimization based on the results obtained from lower-level problem. In this section, a multi-objective optimization model for corridor signal offsets is established to minimize both average travel time and fuel consumption, and then a revised NSGA-II is proposed to identify the set of Pareto-optimal solutions of the optimization model.

#### 4.1. Evaluation indicators for upper-level problem

As discussed in Section 3, the trajectory of each vehicle can be obtained through lower-level simulation for given corridor signal offsets  $\varphi$ . In this study, the vehicular average travel time  $f_t(\varphi)$  and fuel consumption  $f_e(\varphi)$  are used as performance vectors to assess the effectiveness of different corridor signal offsets settings. The values of  $f_t(\varphi)$  and  $f_e(\varphi)$  are determined based on the trajectories of the vehicles, calculated as follows:

$$f_t(\boldsymbol{\varphi}) = \frac{1}{N_{sim}} \sum_{n=1}^{N_{sim}} f_{t,n}(\boldsymbol{\varphi}), f_e(\boldsymbol{\varphi}) = \frac{1}{N_{sim}} \sum_{n=1}^{N_{sim}} f_{e,n}(\boldsymbol{\varphi})$$
(21)

where  $N_{sim}$  represents the total number of vehicles in the lower-level simulation,  $f_{t,n}(\varphi)$  and  $f_{e,n}(\varphi)$  denote the travel time and fuel consumption of n-th simulated vehicle.

The travel time of the n-th vehicle  $f_{t,n}(\varphi)$  can be readily calculated based on the length of its trajectory. However, the average fuel

consumption  $f_{e,n}(\varphi)$  need to be estimated using an appropriate model. In line with previous studies [18,19,25], this paper adopts the fuel consumption model developed by the Australian Road Research Board (ARRB):

$$f_{e,n}(\boldsymbol{\varphi}) = \int g(v_n(t), a_n(t))dt$$
 (22)

$$g\left(v,a\right) = \alpha + \begin{cases} \max\{\beta_1 vR_T(v,a) + \beta_2 mva^2, 0\}, ifa \ge 0\\ \max\{\beta_1 vR_T(v,a), 0\}, & otherwise \end{cases}$$
(23)

$$R_T(v,a) = b_1 + b_2 v^2 + ma + mg\theta$$
 (24)

where m represents the mass of one HDV or CAV.  $R_T$  is the total tractive force required to drive the vehicle.  $\alpha, \beta_1$ , and  $\beta_2$  are the parameter relevant to the fuel rate of vehicles.  $b_1$  and  $b_2$  are the parameter relevant to resistance force.  $\theta$  represents the road grade. More details about the value of parameters can refer to [32].

# 4.2. Signal offsets optimization model for urban corridor

In previous research on signal optimization, the objectives primarily revolved around total delay and the efficiency of intersection operations. The typical approach was to select a single objective from these or to create a weighted summation of the chosen objectives [9,20-24]. However, the objectives may conflict with each other, and determining trade-offs between objectives with different units could be challenging. Therefore, the objective of our proposed model is to identify the Pareto-optimal frontier for corridor signal offsets  $\varphi = [\varphi_{1,2}, \varphi_{2,3}, ., \varphi_{N_{inter}-1, N_{inter}}]$  with the aim of minimizing both the average travel time and fuel consumption. The optimization model is formulated as follows:

$$\min f(\boldsymbol{\varphi}) = [f_t(\boldsymbol{\varphi}), f_e(\boldsymbol{\varphi})] \tag{25}$$

Subject to

$$f_t(\varphi) = \frac{1}{N_{sim}} \sum_{n=1}^{N_{sim}} f_{t,n}(\varphi), f_e(\varphi) = \frac{1}{N_{sim}} \sum_{n=1}^{N_{sim}} f_{e,n}(\varphi)$$
(26)

$$f_{i,n}(\boldsymbol{\varphi}), f_{e,n}(\boldsymbol{\varphi})$$
 is given by lower – level simulation (27)

$$0 \le \varphi_{i,i+1} \le t_C, i = 1, 2.N_{inter} - 1 \tag{28}$$

$$\varphi_{i,i+1} \in N, i = 1, 2.N_{inter} - 1$$
 (29)

where  $\varphi_{i,i+1}$  represents the signal offset between intersection i and i+1. Eq. (28) states the lower and upper boundary of signal offsets. The parameter  $N_{sim}$  is determined for given V/C ratio  $\gamma$ , the saturation time headway  $t_{hw}$ , signal parameters  $[t_G, t_Y, t_R]$ , simulation time horizon  $T_{sim}$ , and CAV penetration rate  $\lambda$ .

### 4.3. Solution algorithm

The optimization model proposed in Section 4.2 is not only a multi-objective optimization model, but also a bi-level programming model. The lower-level problem is resolved through microscopic simulation, making it challenging to precisely solve the optimization model using exact methods. As a widely used metaheuristic method for multi-objective optimization, the Non-Dominated Sorting Genetic Algorithm II (NSGA-II) is viable to obtain a Pareto frontier for objective functions [33]. However, a direct mapping from decision variables  $\varphi$  to objective functions  $f(\varphi)$  is required for the original NSGA-II, whereas the mapping from  $\varphi$  to  $f(\varphi)$  is obtained indirectly by the trajectory of vehicles in our study. In that case, a revised NSGA-II combined with a microscopic simulation for the lower-level problem is proposed to obtain the Pareto-optimal solutions of the proposed optimization model. For given hyperparameters (the size of population M, the maximum number of iteration W, and the probabilities of crossover  $p_c$  and mutation  $p_m$ ), the main steps of the revised NSGA-II consist of the following main steps:

Step 1 Population initialization: For each corridor signal offsets  $\boldsymbol{\varphi}^j = [\varphi^j_{1,2}, \varphi^j_{1,2}, ., \varphi^j_{N_{luner}-1,N_{luner}}]$  of j-th chromosomes in population M, assuming  $\varphi^j_{i,i+1}$  ( $i=1,2,.,N_{inter}-1,j=1,2,.,M$ ) as continuous variables, using a uniform randomness number  $u_{ij}$  from [0,1] to generate  $\varphi^j_{i,i+1}$ , i.e.,  $\varphi^j_{i,i+1} = 0 + u_{ij}(t_C - 0)$ . Then fix  $\varphi^j_{i,i+1}$  to an integer variable by round function, and obtain the initial parent population  $U_0 = [\boldsymbol{\varphi}^1, \boldsymbol{\varphi}^2, ., \boldsymbol{\varphi}^M]$ . The initial child population  $V_0$  is generated using the same method. Set the number of iterations to zero, i.e., w = 0.

Step 2 Non-dominated sorting: Merge  $U_w$  and  $V_w$  into a population  $\mathbf{Z}_w$  of size 2 M, i.e.,  $\mathbf{Z}_w = U_w \cup V_w$ . Each element  $\varphi$  in  $\mathbf{Z}_w$  represents a feasible solution for the upper-level optimization model. For each element  $\varphi^j$ , j=1,2,..,2M, evaluate the vector of objectives  $f^j = [f_t^j, f_e^j]$  (i.e., the average travel time and fuel consumption) based on the lower-level problem simulation (Algorithm 1) and Eqs. (21)-(24). Obtain the objective vector  $\mathbf{F}_w = [f^1, f^2, .., f^{2M}]$  for population  $\mathbf{Z}_w$ . Then, implement the fast-non-dominated-sorting for

population  $Z_w$  to classify all chromosomes  $\varphi^j$ , j = 1, 2, ..., 2M into different dominance levels  $R_d$  (d = 1, 2, ...) (i.e., Pareto ranks and Pareto fronts). Calculate the crowding distance  $D_{jd}$  of j-th chromosome in dominance level  $R_d$ . More details for the achievement of fast-non-dominated sorting and crowding-distance-assignment can be found in [33].

**Step 3 Population selection:** Use tournament method to select the new parent population  $U_{w+1}$  from  $Z_w$ . Note that the size of  $Z_w$  is 2 M, hence only half of  $Z_w$  will be chosen to the new population  $U_{w+1}$ . Firstly, select chromosomes in  $Z_w$  based on the ascending order of dominance levels  $R_d$  (d=1,2,.). Then, for chromosomes in the same dominance levels  $R_d$  (d=1,2,.), select chromosomes in population  $Z_w$  in descending order of crowding distance  $D_{id}$ .

Step 4 New population generation: Set the child population  $V_{w+1}$  to an empty set, i.e.,  $V_{w+1} = \emptyset$ . Randomly select two chromosomes  $\varphi_1, \varphi_2$  from population  $U_{w+1}$ , and generate a rand number  $\omega$  from [0,1], i.e.,  $\omega \sim U(0,1)$ . If  $\omega$  is less than the crossover probability  $p_c$  (i.e.,  $\omega \leq p_c$ ), performing the simulated binary crossover operator to generate two new chromosomes  $\widetilde{\varphi}_1, \widetilde{\varphi}_2$ , and put them into  $V_{w+1}$ , i.e.,  $V_{w+1} = V_{w+1} \cup [\widetilde{\varphi}_1, \widetilde{\varphi}_2]$ . Generate  $\widetilde{\varphi}_1, \widetilde{\varphi}_2$  repeatedly until the size of population  $V_{w+1}$  reaches M. Then, for each chromosome  $\widetilde{\varphi}^j, j = 1, 2, ..., M$  in  $V_{w+1}$ , obtaining a rand number  $\mu$  from [0,1], i.e.,  $\mu \sim U(0,1)$ . If  $\mu$  is less than the mutation probability  $p_m$  (i.e.,  $\mu \leq p_m$ ), performing the polynomial mutation operator to create a new chromosome  $\widetilde{\varphi}^j$ , and replacing the old one, i.e.,  $\widetilde{\varphi}^j = \widetilde{\varphi}^j$ . More details on simulated binary operator and polynomial mutation operator can be found in [34].

**Step 5 Termination Criterion:** Stop the iteration if the number of iteration w reaches the maximum generation W and output the parent population  $U_w$ , otherwise set w = w + 1 and go back to **Step 2**.

For a clear description, the brief pseudo-code is designed for the revised NSGA-II illustrated in Algorithm 2.

Algorithm 2. Brief realization of the revised NSGA-II.

```
Input: The size of population M, the maximum iterations W, the probabilities of crossover p_c and mutation p_m
1: Generate the initial parent population U_0 and child population V_0 randomly.
2: Set w = 0.
3: while w \le W do
     ## Non-dominated sorting
4:
5:
     Set Z_w = U_w \cup V_w.
6:
     Evaluate F_w for population Z_w by Eqs. (21) ~ (24) based on Algorithm 1.
                                                                                                   # Lower-level simulation
7:
     Determine R = \text{fast-non-dominated-sorting}(Z_w, F_w).
8:
     ## Population selection
     Set U_{w+1} = \emptyset and d = 1.
9:
     while |U_{w+1}| + |R_d| \le M do
                                                                # put R_d into new parent population U_{w+1} if available
10:
      Update U_{w+1} = U_{w+1} \cup R_d.
11:
12:
      Set d = d + 1.
13:
     end while
     Determine D_{di} = crowing-distance-assignment (R_d).
14:
15: Sort R_d in descending order of D_{dj}.
16: Update U_{w+1} = U_{w+1} \cup R_d [1:(M-|U_{w+1}|)].
                                                                                   # Put R_d as order of D_{di} into U_{k+1}
17: | ## New population generation
   Set V_{w+1} = \emptyset.
18:
     Generate V_{w+1} = make-new-pop (U_{w+1}). # Use selection, crossover, and mutation to create new population V_{w+1}
19:
20: Set w = w + 1.
21: end while
Output: The set of Pareto-optimal solutions U_{w}
```

# 5. Numerical results and sensitivity analyses

The multi-objective coordinated control strategy for mixed traffic in urban corridors is evaluated through microscopic simulation. Simulation experiments are performed on a personal computer with a 2.10 GHz Intel(R) Core (TM) i7–12700 processor and 16 GB RAM, using Matlab R2023a. The selected case study involves a corridor with three single-lane roadway signalized intersections, and all intersections are equipped with the same signal parameters. The critical parameters used in this study are listed in Table 2 [19,24,25, 29].

**Table 2**Critical parameters in simulation setup.

Parameter	value
Corridor parameters	
Number of intersections $N_{inter}$	3
Length of intersection $L$ (m)	400, 450, 450
Road slope $\theta$ (rad)	0
V/C ratio γ	2/3
The simulation time step $\Delta t$ (s)	1
The simulation time horizon $T_{sim}$ (s)	300
Signal Phase information	
Length of signal cycle $t_C$ (s)	60
Length of green phase $t_G$ (s)	30
Length of yellow phase $t_Y$ (s)	3
Length of red phase $t_R$ (s)	27
Lost time at the beginning of green phase $t_{ls}$ (s)	3
Variables in CAV eco-driving and IDM parameters	
Safety time headway of vehicle $T_{HDC}$ , $T_{ACC}$ , $T_{CACC}$ (s)	1.5, 1.3, 0.9
Saturation flow rate of IDM $t_{hw}$ (s/veh)	2.0
Minimum safety gap $s_0$ (m)	2.0
Length of vehicle l (m)	6.0
Limit speed of vehicle $v_{max}$ (m/s)	18.0
Initial speed of vehicle (m/s)	10.0
Upper bound of CAV acceleration $a_{\text{max}}$ (m/s <sup>2</sup> )	2.5
Desired deceleration of HDV $a_{comf}$ (m/s <sup>2</sup> )	-2.0
Lower bound of CAV acceleration $a_{\min}$ (m/s <sup>2</sup> )	-4.0
Limit changing rate of acceleration $k_{\text{max}}$ (m/s <sup>3</sup> )	10.0

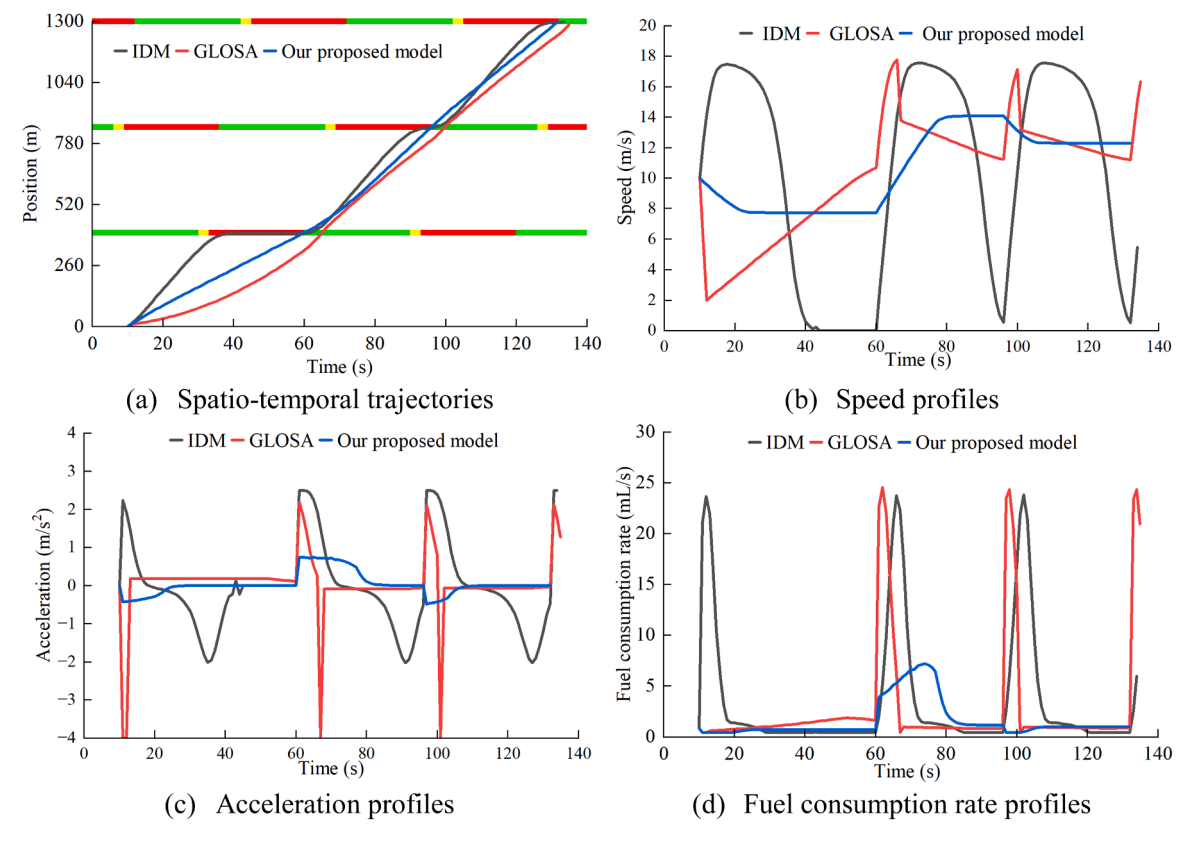


Fig. 6. Comparison of IDM, GLOSA, and the proposed model.

# 5.1. The benefits of the proposed eco-driving strategy in single-vehicle simulation

To illustrate the benefits of the proposed eco-driving strategy, a simulation for a single-vehicle environment is performed. The lengths of intersections are 400, 450, 450 m, respectively. The signal of the first intersection begins in the green phase at t=0 s, and the signal offsets for intersections  $\varphi_{1,2}$ ,  $\varphi_{2,3}$  are configured as 36 s. The initial speed of the vehicle is set to 10.0 m/s, and the vehicle's arrival time is set to t=10 s. It is assumed that a sub-control center within each intersection that collects real-time vehicle state and SPaT information to provide eco-acceleration for each CAV.

The performance of the proposed eco-driving strategy is compared with IDM (described in Section 3.2) and a widely used eco-driving strategy called the Green Light Optimal Speed Advisory (GLOSA) algorithm [35]. The core concept of the GLOSA is to provide acceleration guidance based on SPaT and the current state of the ego vehicle. This guidance aims to help the CAV reach the desired speed while considering the safety conditions related to signal phase changes. Based on GLOSA, the CAV can achieve a trajectory that minimizes delay with safety constraints. More detailed information about the GLOSA can refer to [35].

Fig. 6 depicts the spatio-temporal trajectories, speed profiles, acceleration profiles, and fuel consumption of the three models. Note that the vehicle arrivals at t=10 s, hence the signal phase of the first intersection will turn to red after 23 s. If the vehicle starts with maximum speed (i.e., 18 m/s), the passage time in the first intersection is approximately 22.2 s, which is close to the time that the signal phase turns to red. Therefore, the ego vehicle is unable to pass through the first intersection with an initial speed of 10 m/s. As shown in Fig. 6(a) and (b), the IDM method comes to a stop at intersections, whereas both the GLOSA and our proposed method enable to pass through the intersections without stopping. However, the ego vehicle employed with GLOSA fails to achieve passing intersections at the beginning of the green light time to mitigate the start-up lost time, as our proposed model does. This limitation arises from the safety constraints that dictate the transition of signal phases. GLOSA is compelled to maintain a safe distance when the green phase begins, which results in a delay in its passage through the intersection. Consequently, the GLOSA exhibits a longer travel time in comparison to IDM and our proposed model. On the other hand, as depicted in Fig. 6(c), the acceleration profile of our proposed model exhibits a smoother trend compared to GLOSA and IDM. This smoother acceleration profile effectively prevents abrupt changes in speed, leading to reduced fuel consumption, as indicated in Fig. 6(d).

Furthermore, to eliminate the bias of energy consumption models towards the efficacy of our eco-driving strategy. Expect the ARRB model, the VT-Micro [36], and the electric vehicle energy consumption (EVEC) model [37] are also selected to validate the effectiveness of our proposed model at different arrival times, as shown in Table 3. The results show that our proposed model obtains the minimum travel time. In part of energy consumption, our proposed model outperforms the IDM and GLOSA in both ARRB, VT-micro, and EVEC models.

# 5.2. The efficiency of coordinated control strategy

The parameters of corridor simulation for mixed traffic are outlined in Table 2, the V/C ratio is set at 2/3, and the CAV PR is set to 0.6. The arrival interval of vehicles is random. For the revised NSGA-II, the size of population M = 80, the maximum number of iterations W = 32, and the probabilities of crossover  $p_c = 0.9$  and mutation  $p_m = 0.1$ . Based on the setup, the coordinated control strategy is executed. To mitigate the influence of random arrival intervals, the AFC and ATT for each solution of signal phase offsets are obtained by averaging 20 times Monte Carlo simulations.

Regarding the convergence of NSGA-II, Fig. 7(a) depicts the value of objective functions with each dual iteration. The grand truth value is derived through an exhaustive method, involving total feasible solutions of  $t_C \times t_C$ . Consequently, the lower-level problem of the exhaustive method necessitates 3600 simulation runs. It is found that, in comparison to the objective function values of the initial population (w = 0), both the AFC and ATT exhibit notable reductions as the number of iterations increases. By the time the iteration count reaches w = 16, the Pareto-optimal frontier closely approximates the truth value. Notably, the simulation efforts required by NSGA-II are merely half of those needed by the exhaustive method, with the simulation count for NSGA-II being (w + 1) × M = 1360. Moreover, to demonstrate the stability of the revised NSGA-II, the numerical experiment has been run 5 times with different initial populations independently. The objective functions of Pareto-optimal solution sets for each run have been illustrated in Fig. 7(b). The Result shows that the Pareto-optimal solution sets for each run close to the ground truth value, namely different initial population produces the same Pareto-optimal frontier. This result validates the stability of the revised NSGA-II.

As shown in Fig. 7(a), two boundary values on the truly Pareto frontier are discernible, denoting the minimum achievable AFC and ATT values. These are referred to as the optimal AFC and optimal ATT, respectively. The effectiveness of the proposed coordinated control strategy is assessed by comparing the spatio-temporal trajectories of optimal ATT and AFC, as depicted in Fig. 8. The trajectory of HDVs is represented by the solid black line, while the trajectory of CAVs is depicted by the solid blue line. It can be found that the signal offsets in the optimal ATT scenario are lower than those in the optimal AFC scenario, i.e., the signal offsets of the optimal ATT scenarios are [23,27] s, whereas the optimal AFC are [50] s. The trajectories of optimal ATT and AFC coincide within the first intersection. Consequently, the terminal speed at which the first CAV passes through the first intersection is about 7.7 m/s, as depicted in Fig. 6(b). In the optimal AFC scenario, the average speed of the ego CAV within the second intersection is calculated as 450/50 = 9 m/s, as shown in Fig. 8(b). Therefore, the speed of the ego vehicle and its following vehicles undergo only marginal changes compared to the optimal ATT scenario, resulting in a significant reduction in fuel consumption as displayed in Fig. 7(b) (from 263.6 mL to 222.7 mL). However, this decrease in fuel consumption is a trade-off by an increase in travel time when compared to the optimal ATT scenario (from 90.2 s to 130.2 s).

#### 5.3. Sensitivity analysis to CAV PR

Fig. 9 presents the Pareto-optimal frontier for average travel time and fuel consumption with different CAV PR, it is observed that with an increase in CAV PR, the Pareto-optimal frontier exhibits an overall trend of moving towards the lower left direction in the objective functions' plane composed of ATT and AFC. This phenomenon indicates that the solutions of the Pareto-optimal frontier with lower CAV PR are almost dominated by the solutions with higher CAV PR. In other words, for any solution within the lower CAVPR, superior solutions in terms of both AFC and ATT can invariably be found within the higher CAV PR. This observation underscores that the coordinated control strategy involving corridor signal offset optimization and CAV's eco-driving enhances efficiency and energy savings within mixed traffic flow.

Moreover, the optimal AFC and ATT with different CAV PR are given in Table 4. The values of optimal AFC and ATT exhibit a decreasing trend as CAV PR increases, the maximum reduction in optimal ATT is 2.3% (decreasing from 90.8 s to 88.7 s), and the optimal AFC is reduced by 32.2% maximum (decreasing from 279.1 mL to 189.1 mL). However, the optimal ATT with a CAV PR of 0.2 is longer by 0.2% in comparison to that with a CAV PR of 0.0. This can be attributed to the fact that, when the CAV PR is set to 0.2, the driving mode for CAVs predominantly approaches ACC. This adjustment influences the prediction for passage time as outlined in Section 3.3.1, leading to instances where the predicted passage time is larger than the actual value in certain cases. Specifically, there are situations where a preceding HDV manages to pass the adjacent intersection based on the current signal cycle along with its acceleration and speed. However, according to Eqs. (10) and (11), a driving behavior of constant speed is assumed, thereby making the predicted passage time larger than the actual value. Consequently, this discrepancy results in a longer travel time. Such findings is in line with [24].

# 5.4. Sensitivity analysis to V/C ratio

The V/C ratio holds a significant influence over the execution of the coordinated control strategy. A higher V/C ratio compresses the spatio-temporal resource of vehicles, potentially resulting in increased travel time and fuel consumption for the mixed traffic flow. Fig. 10 depicts the Pareto-optimal frontier under various V/C ratios, with the fixed CAV PR of 0.6. As the V/C ratio increases, the optimal ATT exhibits a rising trend, whereas the optimal AFC demonstrates a decreasing trend. This phenomenon can be attributed to the increase in the number of CAVs as the V/C ratio rises. This increase in CAVs facilitates smoother passage for more HDVs through intersections, consequently leading to a notable reduction in fuel consumption for all vehicles. However, the rise in the V/C ratio also results in the compression of available road space resources for vehicles, leading to a decrease in speed and a rise in travel time.

Furthermore, the values of optimal AFC and ATT with different V/C ratios are given in Table 5. The benchmark scenario, with a CAV PR of 0.0, has been selected for comparison. Notably, both the optimal ATT and AFC values under a CAV PR of 0.6 are all smaller than those in the benchmark scenario (CAV PR is 0.0) This observation underscores the efficacy of the proposed corridor control strategy, achieved through the synergistic implementation of eco-driving strategy, and signal offset optimization. The maximum savings of optimal ATT is 1.5% (decreasing from 94.8 s to 93.4 s), and the optimal AFC is saved by 23.5% maximum (decreasing from 287.9 mL to 220.2 mL).

# 5.5. Sensitivity analysis to joint composition of CAV PR and V/C ratio

The effectiveness of the proposed coordinated control strategy is evaluated with combined consideration of the V/C ratio and CAV PR, as illustrated in Fig. 11. The x-axis denotes the V/C ratio ranging from 1/6 to 6/6 as an interval of 1/6. The y-axis represents the CAV PR ranging from 0.0 to 1.0 as an interval of 0.2. As illustrated in Fig. 11 (a), the optimal ATT exhibits an increase as the V/C ratio rises, similar to the findings in Table 5. Additionally, it is noteworthy that the penetration of CAVs enhances the maximum savings in ATT, escalating from 0.8% to 4.4% with the increase in the V/C ratio. For instance, when the V/C ratio is 1/6, the maximum savings in optimal ATT amount to 0.4% (calculated as  $100 \times (85.7 - 85.0)/85.7$ ), while at the V/C ratio of 6/6, the maximum savings in optimal ATT reach 4.4% (calculated as  $100 \times (101.3 - 96.8)/101.3$ ). This observation underscores the effectiveness of the proposed coordinated control strategy. However, when the value of CAV PR is below 0.4, the optimal ATT still performs a larger value than the non-CAV environment (CAV PR = 0.0) attributed to the conservative estimation of the passage time of the preceding HDV.

Regarding the optimal AFC, as shown in Fig. 11 (b), when the CAV PR surpasses 0.4, the optimal AFC value exhibits a decreasing trend with rising V/C ratios, aligning with the trends noted in Table 5. However, when the CAV PR fall below 0.4, the optimal AFC experiences a decrease firstly, followed by an increase. The lowest value of optimal AFC coincides with a V/C ratio of 5/6. When the value of the V/C ratio is at 5/6, the average travel time reaches to 97.3 s, and the average speed is calculated as 1300/97.3 = 13.4 m/s. Notably, this speed is very close to the eco-cruise speed (i.e., the cruising speed at which vehicles can achieve minimal fuel

**Table 3**Average travel time and energy consumption benefits with different arrival time.

Methods	Travel time (s)	Energy consumption model			
		ARRB (mL)	VT-micro (mL)	EVEC (kJ)	
IDM (benchmark)	94.9	385.7	198.6	698.5	
GLOSA	97.3 (+2.5%)	350.9 (-9.0%)	175.1(-11.8%)	649.4 (-7.0%)	
Our proposed model	93.5 (-1.5%)	229.1 (-40.6%)	139.9 (-29.6%)	576.0 (-17.5%)	

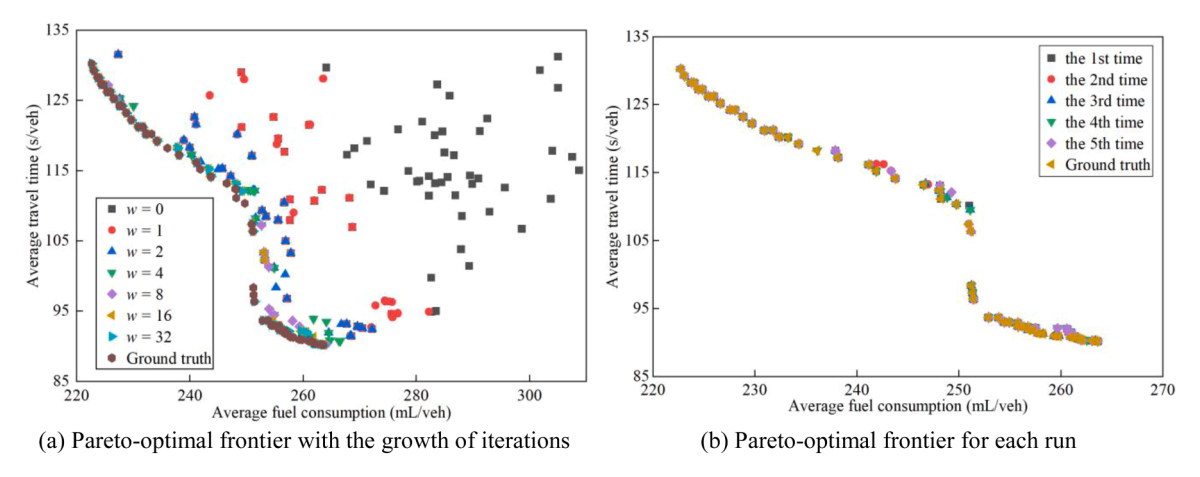


Fig. 7. The convergence and stability of the revised NSGA-II.

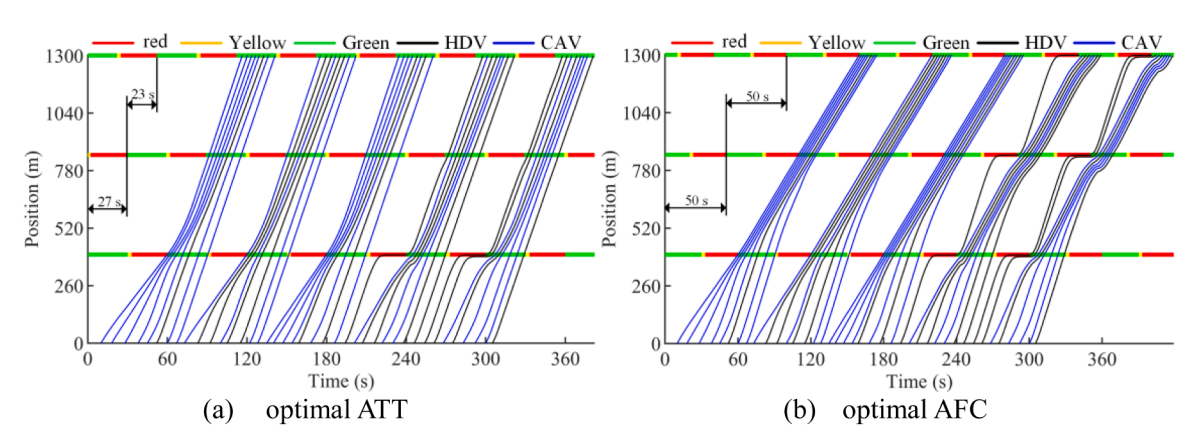


Fig. 8. The spatio-temporal trajectories of optimal ATT and AFC.

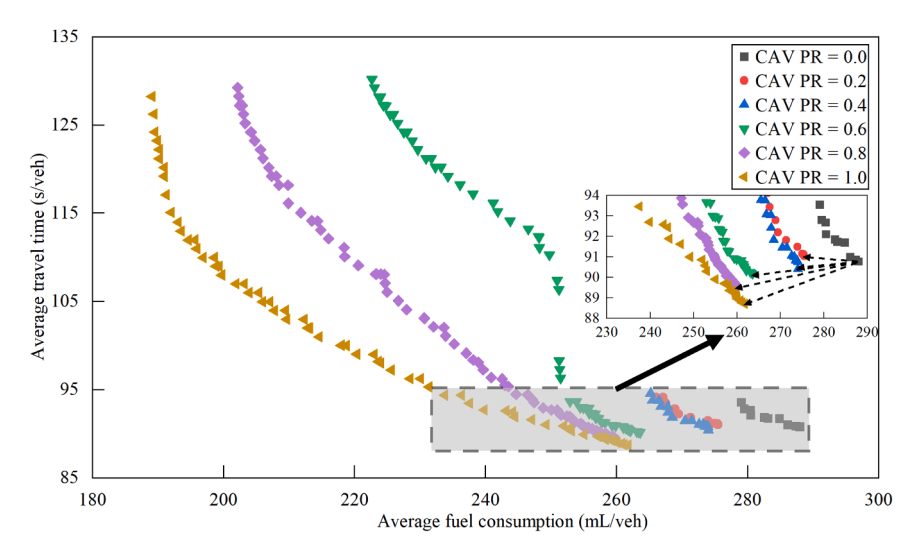


Fig. 9. The Pareto-optimal frontier with different CAV PR.

**Table 4**Optimal ATT and AFC with different CAV PR.

CAV PR	0.0 (benchmark)	0.2	0.4	0.6	0.8	1.0
ATT (s/veh)	90.8	91.0 (+0.2%)	90.4 (-0.4%)	90.2 (-0.7%)	89.5 (-1.4%)	88.7 (-2.3%)
AFC (mL/veh)	279.1	266.1 (-4.7%)	265.2 (-5.0%)	222.7 (-20.2%)	202.2 (-27.4%)	189.1 (-32.2%)

consumption) with a value of 13.3 m/s, as documented in [18]. Additionally, with an increasing V/C ratio, the average travel time related to optimal AFC undergoes a decrease, culminating in the occurrence of the minimum optimal AFC at a V/C ratio of 5/6. Furthermore, the adoption of the proposed coordinated control strategy contributes to notable enhancements in the maximum savings of the AFC. This improvement ranges from 31.9% to 35.9% as the V/C ratio increases. For instance, when the V/C ratio is 1/6, the maximum savings in optimal AFC amount to 31.9% (calculated as  $100 \times (293.5 - 200.5)/293.5$ ), and when the V/C ratio is 6/6 (i.e., fully saturated conditions), the maximum savings in optimal AFC remain at 35.9% (calculated as  $100 \times (287.9 - 184.5)/287.9$ ).

#### 6. Conclusions

This study proposes a multi-objective coordinated control strategy for mixed traffic with partially connected and automated vehicles in urban corridors. To decouple the joint effects of the vehicular driving behaviors and corridor signal offsets setting, a bi-level structure is designed. At the lower-level, three types of driving modes are presented to depict the desired car-following acceleration, and a trigonometry method combined with driving modes is selected to generate the ecological trajectories of CAVs. At the upper-level, a multi-objective optimization model for corridor signal offsets is established to optimize the ATT and AFC based on the lower-level simulations. Additionally, a revised NSGA-II is proposed to determine the set Pareto frontier solutions with different CAV penetration rate (CAV PR). Numerical experiments and sensitivity analysis are conducted to analyze the effectiveness and the generalization of the proposed control strategy. The main conclusion of the study drawn as follows:

- (1) Both the travel time and fuel consumption are reduced by the proposed eco-driving strategy compared with IDM and GLOSA in the single-vehicle simulation;
- (2) The Pareto-optimal solutions with lower CAV PR are dominated by the solutions with higher CAV PR;
- (3) The values of optimal AFC and ATT exhibit a decreasing trend as the CAV PR increases. The maximum savings in optimal ATT reach 2.3%, and for the optimal AFC, the savings amount to 32.2%;
- (4) The optimal ATT with low CAV PR performs a larger value than the non-CAV environment due to a conservative estimation of the passage time of preceding HDV.

Our proposed coordinated control strategy can potentially help the planning of CAV's trajectory and the design of corridor signal offset setting in the future mixed traffic flow environment. However, there are still several limitations in this study: (1) A simple passage time estimation method is used. An estimation method while considering historical information can effectively improve the accuracy of passage time, such as the Kalman filter. (2) A corridor with a single-lane roadway is selected. In the real world, a typical intersection usually consists of multiple incoming lanes, the trajectory planning composited of longitudinal and lateral movement is essential for actual implementation. (3) The optimization model for isolated signalized intersections is not addressed. A more

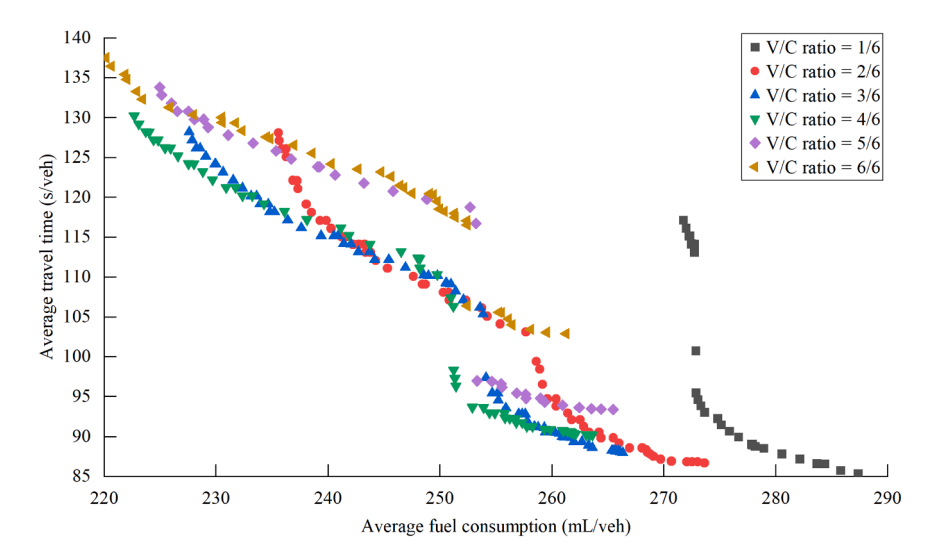


Fig. 10. The Pareto-optimal frontier with different V/C ratio.

**Table 5**Optimal ATT and AFC with different V/C ratio.

V/C ratio	ATT (s/veh)	ATT (s/veh)		AFC (mL/veh)	
	CAV PR = 0.0 (Benchmark)	CAV PR = 0.6	CAV PR = 0.0 (Benchmark)	CAV PR = 0.6	
1/6	85.7	85.4 (-0.4%)	293.5	271.8 (-7.4%)	
2/6	87.0	86.7 (-0.3%)	286.7	235.6 (-17.8%)	
3/6	88.2	88.0 (-0.3%)	281.4	227.6 (-19.1%)	
4/6	90.8	90.2 (-0.7%)	279.1	222.7 (-20.2%)	
5/6	94.8	93.4 (-1.5%)	278.6	225.0 (-19.3%)	
6/6	101.3	100.9 (-0.5%)	287.9	220.2 (-23.5%)	

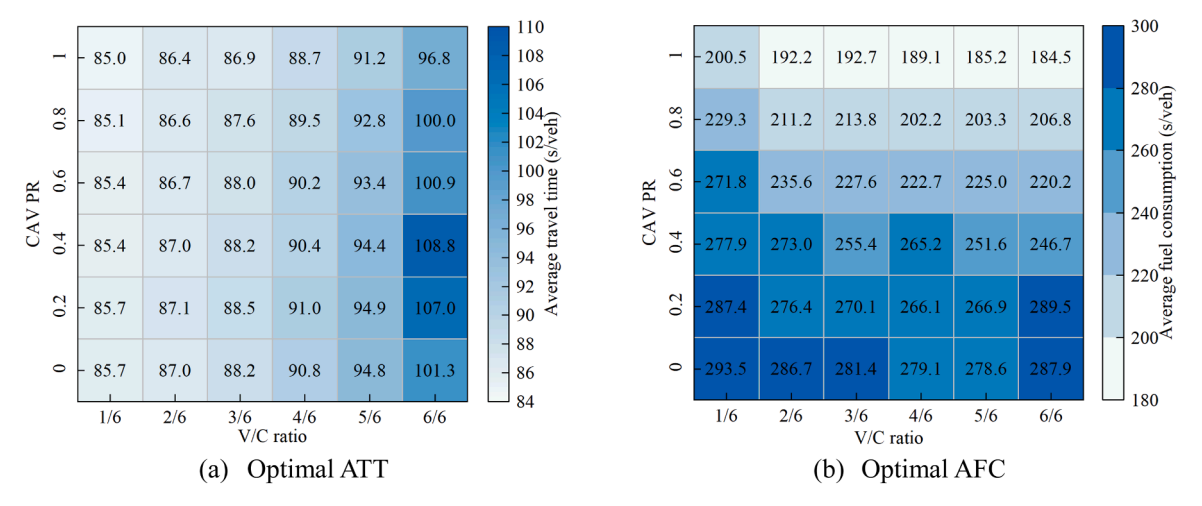


Fig. 11. The values of optimal ATT and AFC with different level of V/C ratio and CAV PR.

comprehensive approach involving cooperative optimization between vehicles, intersections, and urban corridors could potentially yield greater benefits for mixed traffic flow. Further study will consider a more complex and realistic environment for mixed traffic.

## CRediT authorship contribution statement

**Xiaonian Shan:** Conceptualization, Methodology, Validation, Writing – review & editing. **Peng Hao:** Methodology, Writing – review & editing. **Guoyuan Wu:** Writing – review & editing. **Changxin Wan:** Methodology, Writing – original draft.

# **Declaration of Competing Interest**

The authors declare that they have no known competing financial interests or personal relationships that could have appeared to influence the work reported in this paper.

# Data availability

Data will be made available on request.

#### Acknowledgments

This research was supported by the National Natural Science Foundation of China (Grant No. 52002113), the Natural Science Foundation of Jiangsu Province (Grant No. BK20200526), the Key Laboratory of Road and Traffic Engineering of the Ministry of Education, Tongji University (Grant No. K202302), and the Project on Excellent Post-graduate Dissertation of Hohai University.

#### References

- [1] O. US EPA, Inventory of U.S. Greenhouse Gas Emissions and Sinks: 1990–2019, (2021). (https://www.epa.gov/ghgemissions/inventory-us-greenhouse-gas-emissions-and-sinks-1990–2019) (Accessed August 8, 2023).
- [2] Q. Guo, L. Li, X. (Jeff) Ban, Urban traffic signal control with connected and automated vehicles: a survey, Transp. Res. Part C Emerg. Technol. 101 (2019) 313–334, https://doi.org/10.1016/j.trc.2019.01.026.

- [3] Y. Xing, H. Zhou, X. Han, M. Zhang, J. Lu, What influences vulnerable road users' perceptions of autonomous vehicles? a comparative analysis of the 2017 and 2019 Pittsburgh surveys, Technol. Forecast. Soc. Change 176 (2022) 121454, https://doi.org/10.1016/j.techfore.2021.121454.
- [4] J. Li, C. Yu, Z. Shen, Z. Su, W. Ma, A survey on urban traffic control under mixed traffic environment with connected automated vehicles, Transp. Res. Part C Emerg. Technol. 154 (2023) 104258, https://doi.org/10.1016/j.trc.2023.104258.
- [5] A. Alessandrini, A. Campagna, P.D. Site, F. Filippi, L. Persia, Automated vehicles and the rethinking of mobility and cities, Transp. Res. Procedia 5 (2015) 145–160, https://doi.org/10.1016/j.trpro.2015.01.002.
- [6] N. Li, S. Chen, J. Zhu, D.J. Sun, A platoon-based adaptive signal control method with connected vehicle technology, Comput. Intell. Neurosci. 2020 (2020) e2764576, https://doi.org/10.1155/2020/2764576.
- [7] L. Song, W. Fan, Traffic signal control under mixed traffic with connected and automated vehicles: a transfer-based deep reinforcement learning approach, IEEE Access 9 (2021) 145228–145237, https://doi.org/10.1109/ACCESS.2021.3123273.
- [8] Y. Feng, K.L. Head, S. Khoshmagham, M. Zamanipour, A real-time adaptive signal control in a connected vehicle environment, Transp. Res. Part C Emerg. Technol. 55 (2015) 460–473, https://doi.org/10.1016/j.trc.2015.01.007.
- [9] Z. Li, L. Elefteriadou, S. Ranka, Signal control optimization for automated vehicles at isolated signalized intersections, Transp. Res. Part C Emerg. Technol. 49 (2014) 1–18, https://doi.org/10.1016/j.trc.2014.10.001.
- [10] X. (Joyce Liang, S.I. Guler, V.V. Gayah, A heuristic method to optimize generic signal phasing and timing plans at signalized intersections using connected vehicle technology, Transp. Res. Part C Emerg. Technol. 111 (2020) 156–170, https://doi.org/10.1016/j.trc.2019.11.008.
- [11] Q. Wang, Y. Yuan, X. (Terry Yang, Z. Huang, Adaptive and multi-path progression signal control under connected vehicle environment, Transp. Res. Part C Emerg. Technol. 124 (2021) 102965, https://doi.org/10.1016/j.trc.2021.102965.
- [12] K. Yang, S.I. Guler, M. Menendez, Isolated intersection control for various levels of vehicle technology: conventional, connected, and automated vehicles, Transp. Res. Part C Emerg. Technol. 72 (2016) 109–129, https://doi.org/10.1016/j.trc.2016.08.009.
- [13] M. Morari, J. H. Lee, Model predictive control: past, present and future, Comput. Chem. Eng. 23 (1999) 667–682, https://doi.org/10.1016/S0098-1354(98)
- [14] W. Zhao, D. Ngoduy, S. Shepherd, R. Liu, M. Papageorgiou, A platoon based cooperative eco-driving model for mixed automated and human-driven vehicles at a signalised intersection, Transp. Res. Part C Emerg. Technol. 95 (2018) 802–821, https://doi.org/10.1016/j.trc.2018.05.025.
- [15] H. Yao, X. Li, Decentralized control of connected automated vehicle trajectories in mixed traffic at an isolated signalized intersection, Transp. Res. Part C Emerg. Technol. 121 (2020) 102846, https://doi.org/10.1016/j.trc.2020.102846.
- [16] Z. Wang, G. Wu, M.J. Barth, Cooperative eco-driving at signalized intersections in a partially connected and automated vehicle environment, IEEE Trans. Intell. Transp. Syst. 21 (2020) 2029–2038. https://doi.org/10.1109/TITS.2019.2911607.
- [17] X. Han, R. Ma, H.M. Zhang, Energy-aware trajectory optimization of CAV platoons through a signalized intersection, Transp. Res. Part C Emerg. Technol. 118 (2020) 102652, https://doi.org/10.1016/j.trc.2020.102652.
- [18] M. Yu, J. Long, An eco-driving strategy for partially connected automated vehicles at a signalized intersection, IEEE Trans. Intell. Transp. Syst. 23 (2022) 15780–15793. https://doi.org/10.1109/TITS.2022.3145453.
- [19] Y. Hu, P. Yang, M. Zhao, D. Li, L. Zhang, S. Hu, W. Hua, W. Ji, Y. Wang, J. Guo, A generic approach to eco-driving of connected automated vehicles in mixed urban traffic and heterogeneous power conditions, IEEE Trans. Intell. Transp. Syst. (2023) 1–18, https://doi.org/10.1109/TITS.2023.3286441.
- [20] H. Jung, S. Choi, B.B. Park, H. Lee, S.H. Son, Bi-level optimization for eco-traffic signal system, Int. Conf. Connect. Veh. Expo. (ICCVE) 2016 (2016) 29–35, https://doi.org/10.1109/ICCVE.2016.6.
- [21] B. Xu, X.J. Ban, Y. Bian, W. Li, J. Wang, S.E. Li, K. Li, Cooperative method of traffic signal optimization and speed control of connected vehicles at isolated intersections, IEEE Trans. Intell. Transp. Syst. 20 (2019) 1390–1403, https://doi.org/10.1109/TTTS.2018.2849029.
- intersections, IEEE Trans. Intell. Transp. syst. 20 (2019) 1390–1403, https://doi.org/10.1109/1115.2018.2849029.

  [22] Z. Yao, B. Zhao, T. Yuan, H. Jiang, Y. Jiang, Reducing gasoline consumption in mixed connected automated vehicles environment: a joint optimization framework for traffic signals and vehicle trajectory, J. Clean. Prod. 265 (2020) 121836, https://doi.org/10.1016/j.jclepro.2020.121836.
- [23] M. Tajalli, A. Hajbabaie, Traffic signal timing and trajectory optimization in a mixed autonomy traffic stream, IEEE Trans. Intell. Transp. Syst. 23 (2022) 6525–6538, https://doi.org/10.1109/TITS.2021.3058193.
- [24] Z. Yang, Y. Feng, H.X. Liu, A cooperative driving framework for urban arterials in mixed traffic conditions, Transp. Res. Part C Emerg. Technol. 124 (2021) 102918, https://doi.org/10.1016/j.trc.2020.102918.
- [25] H. Jiang, J. Hu, S. An, M. Wang, B.B. Park, Eco approaching at an isolated signalized intersection under partially connected and automated vehicles environment, Transp. Res. Part C Emerg. Technol. 79 (2017) 290–307, https://doi.org/10.1016/j.trc.2017.04.001.
- [27] A. Talebpour, H.S. Mahmassani, Influence of connected and autonomous vehicles on traffic flow stability and throughput, Transp. Res. Part C Emerg. Technol. 71 (2016) 143–163, https://doi.org/10.1016/j.trc.2016.07.007.
- [28] D. Ngoduy, Analytical studies on the instabilities of heterogeneous intelligent traffic flow, Commun. Nonlinear Sci. Numer. Simul. 18 (2013) 2699–2706, https://doi.org/10.1016/j.cnsns.2013.02.018.
- [29] Z. Yao, R. Hu, Y. Wang, Y. Jiang, B. Ran, Y. Chen, Stability analysis and the fundamental diagram for mixed connected automated and human-driven vehicles, Phys. A Stat. Mech. Appl. 533 (2019) 121931, https://doi.org/10.1016/j.physa.2019.121931.
- [30] S. Cui, F. Cao, B. Yu, B. Yao, Modeling heterogeneous traffic mixing regular, connected, and connected-autonomous vehicles under connected environment, IEEE Trans. Intell. Transp. Syst. 23 (2022) 8579–8594, https://doi.org/10.1109/TITS.2021.3083658.
- [31] H. Xia, K. Boriboonsomsin, M. Barth, Dynamic eco-driving for signalized arterial corridors and its indirect network-wide energy/emissions benefits, J. Intell. Transp. Syst. 17 (2013) 31–41, https://doi.org/10.1080/15472450.2012.712494.
- [32] R. Akcelik, Efficiency and drag in the power-based model of fuel consumption, Transp. Res. Part B Methodol. 23 (1989) 376–385, https://doi.org/10.1016/0191-2615(89)90014-3.
- [33] K. Deb, A. Pratap, S. Agarwal, T. Meyarivan, A fast and elitist multiobjective genetic algorithm: NSGA-II, IEEE Trans. Evolut. Comput. 6 (2002) 182–197, https://doi.org/10.1109/4235.996017.
- [34] K. Deb, S. Agrawal, A Niched-Penalty Approach for Constraint Handling in Genetic Algorithms, in: A. Dobnikar, N.C. Steele, D.W. Pearson, R.F. Albrecht (Eds.), Artificial Neural Nets and Genetic Algorithms, Springer, Vienna, 1999: pp. 235–243. https://doi.org/10.1007/978-3-7091-6384-9\_40.
- [35] S. Stebbins, M. Hickman, J. Kim, H.L. Vu, Characterising green light optimal speed advisory trajectories for platoon-based optimisation, Transp. Res. Part C Emerg. Technol. 82 (2017) 43–62, https://doi.org/10.1016/j.trc.2017.06.014.
- [36] X. Li, J. Cui, S. An, M. Parsafard, Stop-and-go traffic analysis: theoretical properties, environmental impacts and oscillation mitigation, Transp. Res. Part B: Methodol. 70 (2014) 319–339, https://doi.org/10.1016/j.trb.2014.09.014.
- [37] X. Wu, D. Freese, A. Cabrera, W.A. Kitch, Electric vehicles' energy consumption measurement and estimation, Transp. Res. Part D Transp. Environ. 34 (2015) 52–67, https://doi.org/10.1016/j.trd.2014.10.007.